18

Monitoring the Intertidal Environment with Biomimetic Devices

Fernando P. Lima[1,2], Nicholas P. Burnett[1], Brian Helmuth[1], Nicole Kish[1], Kyle Aveni-Deforge[1] and David S. Wethey[1]
[1]*Department of Biological Sciences, 715 Sumter Street*
University of South Carolina, Columbia, South Carolina 29208
[2]*CIBIO, Centro de Investigação em Biodiversidade e Recursos Genéticos*
Campus Agrário de Vairão, 4485-661 Vairão
[1]*United States of America*
[2]*Portugal*

1. Introduction

Worldwide, the narrow bands of habitat between the tidemarks on coastal shores are inhabited by a variety of marine species which periodically have to cope with stressful terrestrial conditions during low tide (Raffaelli & Hawkins, 1996; Denny & Wethey, 2000; Harley, 2008). The interplay between biotic and abiotic factors acting over such small spatial scales results in outstandingly condensed and diverse communities, which are regarded as ideal natural models for studying the coupled role of physical and biological factors in determining the abundance and distribution of organisms (Raffaelli & Hawkins, 1996).

Most intertidal invertebrates and algae are sessile or slow moving and cannot prevent being exposed to extreme stressful events, and thus are recognized as sensitive indicators of the effects of climate variability and climate change (Helmuth et al., 2006 and references within). Subsequently, temperature-driven mass mortalities of intertidal organisms such as limpets, mussels and barnacles have been observed in the field after exposure to periods of acute thermal stress (e.g., Lewis, 1954; Connell, 1961a; Crisp, 1964; Harley, 2008; Jones et al., 2010). Importantly, molecular and physiology studies have also recently shown the importance of sub-lethal stresses in shaping the distribution of intertidal species (e.g., Somero, 2002; Dahlhoff, 2004; Sorte & Hofmann, 2004; Helmuth et al., 2005).

In addition to clines in thermal stress, the tidal cycle also generates steep gradients in light, oxygen and nutrient availability, wave force, salinity and desiccation. These abiotic factors have long been identified as drivers in the physiology and ecology of intertidal animals and plants (Broekhuysen, 1941; Smaldon & Duffus, 1984; Denny & Wethey, 2000; Santini et al., 2001; Firth & Williams, 2009). Vertical clines in the strength of stressors, determined by the timing and duration of emersion/submersion (Foster, 1971) were firstly regarded as the main causative factors for the ubiquitous vertical substitution of species observed at scales of a few meters on rocky shores (Stephenson & Stephenson, 1949; Lewis, 1964). Soon after, results from experimental ecology began to demonstrate the importance of biotic, selective pressures related to competition, predation, grazing, and recruitment in setting zonation

patterns (Connell, 1961b; Hawkins et al., 1992). Connell (1972) suggested that the lower distributional limits of intertidal organisms were frequently set by biological interactions, while the upper limits were often set by desiccation and thermal factors. Later on, some authors showed that the strengths of some biotic interactions were themselves influenced by gradients in abiotic stress (Hodkinson, 1999; Wethey, 2002; Pincebourde et al., 2008; Yamane & Gilman, 2009).

2. Monitoring the environment at the scale of the organisms

Recent advances in remote sensing and information technology, allied to the creation of huge data repositories, have provided the large volumes of environmental data needed to feed bio-climatic or process-based models, and thus have fueled numerous large-scale studies relating biogeographic patterns of intertidal organisms with changes in climate (e.g., Lima et al., 2007a; Lima et al., 2007b; Wethey & Woodin, 2008; Berke et al., 2010; Jones, et al., 2010). It has become apparent, however, that these large-scale studies may be missing key environmental features only observed at the scale of the organisms (Helmuth et al., 2010). For example, when intertidal organisms are submerged, their body temperatures are in equilibrium with the surrounding water, but during aerial exposure other factors such as air temperature, wind speed, solar radiation and relative humidity come into play, interacting with the physical characteristics of the organisms such as their thermal inertia (Spotila et al., 1973), shape and color (Helmuth, 1999; Denny et al., 2006; Gilman et al., 2006) to determine the organism's body temperature. As a result, daily variations in body temperature can exceed 20ºC (Helmuth & Hofmann, 2001; Helmuth, 2002; Helmuth, et al., 2010), a range that is far greater than the yearly variation of coastal sea temperature at most locations. Daily variations in temperature may also be radically different between individuals just a few meters apart but located in surfaces facing different directions (Helmuth, 1998; 2002; Wethey, 2002; Helmuth, et al., 2005; Harley, 2008; Lima & Wethey, 2009), and can depart significantly from measurements of air and surface temperature. Topography interacts with daily and seasonal variation in the incidence of sunlight, tide and weather, modifying heat exchanges between organisms and the environment, leading to large-scale geographic mosaics of thermal and desiccation stress (Gilman, et al., 2006; Helmuth, et al., 2006). Such topographic variation in stress has dramatic consequences for the distribution of species and for the intensity of their interactions (Wethey, 1984; 2002). Local, small-scale topography also strongly influences wave exposure. Wave forces are one of the major sources of natural disturbance in rocky shores, by directly creating patchiness by dislodging organisms (Sousa, 1984), by underpinning thermal regimes of organisms, by inducing behavioral responses that facilitate body temperature cooling (Fitzhenry et al., 2004), or by altering the timing of submersion (Harley & Helmuth, 2003).

Thus, although it is clear that environmental data at the scale of the organisms should be explicitly used when describing, modeling and predicting biogeographic and ecological changes within these ecosystems, this requirement has been hindered by the lack of cost-effective, self-contained instruments that can measure physiologically relevant aspects of the environment at the scale of the organisms. Here we describe four types of biomimetic sensors/loggers, specifically designed to capture different aspects of the coastal environment. These devices can be used to measure and log temperature, water loss (desiccation) and wave forces in the intertidal, as perceived by intertidal organisms.

3. Biomimetic temperature data loggers: robomussels and robolimpets

In the intertidal environment, the most important abiotic determinant of organismal performance and distribution from micro to macroscales is indubitably temperature (Southward, 1958; Crisp, 1964; Lewis, 1964; Southward, 1995; Denny & Wethey, 2000; Helmuth & Hofmann, 2001; Gilman, et al., 2006; Wethey & Woodin, 2008).

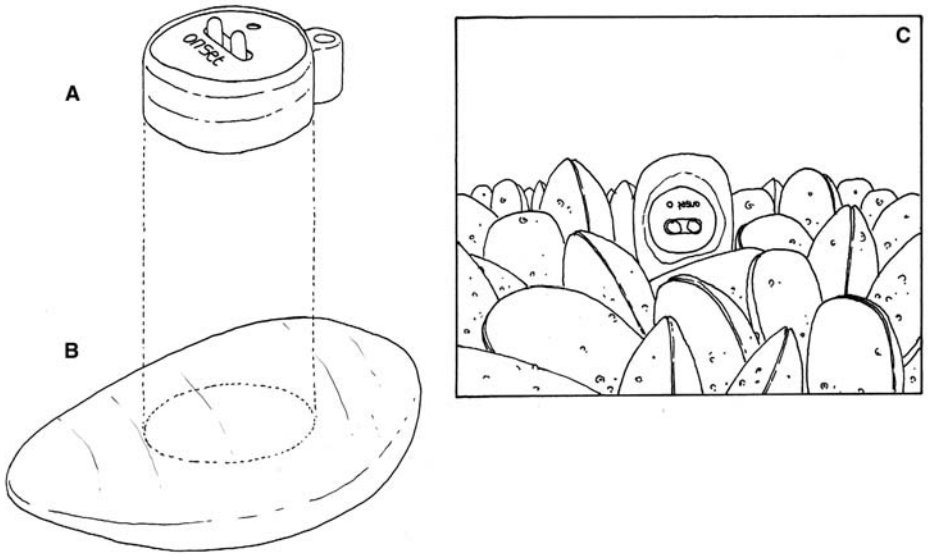

Fig. 1. Temperature logger mimicking a *Mytilus californianus* (robomussel). A: Onset TidbiT logger, B: Evercoat Everfix epoxy cast of a *M. californianus*, C: representation of a robomussel deployed in a mussel bed in the field.

Until recently, measuring body temperatures in the intertidal zone was inefficient or even impracticable at large spatial or temporal scales, as temperature loggers were too expensive, large, and required frequent servicing. The harshness of the intertidal zone, associated with rapidly varying temperatures, tremendous wave forces and hard substrata, was also problematic, often causing the loss of sensors and data loggers. Recent advances in sensor miniaturization resulted in a series of commercially-available data loggers that were rapidly adopted by intertidal ecologists and physiologists. Unfortunately, little consideration was given to what these instruments were actually measuring. As is true for organisms, the color, morphology, and mass of a temperature logger can significantly affect the temperature that it records. As a result, without carefully considering the characteristics of the instrument being deployed, a datalogger may easily record temperatures that have very little to do with the organism of interest. Instead, one must use *biomimetic* sensors-instruments specifically matched to the physical characteristics of the organism, in this case case to the thermal characteristics. To overcome these problems, two types of biomimetic sensors/loggers have been developed: robomussels (Helmuth & Hofmann, 2001; Fitzhenry, et al., 2004) and robolimpets (Lima & Wethey, 2009). These are self-contained, rugged and

miniaturized devices that can be easily and inexpensively built to mimic the thermal characteristics of intertidal organisms and record their thermal trajectories over a broad variety of temporal and spatial scales. Robomussels and robolimpets are biomimetic in the sense that they feature the thermal characteristics and visually resemble real organisms, being inconspicuous in the intertidal environment and thus less likely to be intentionally destroyed.

Robomussels (Fig. 1) are constructed following the methods described by Fitzhenry et al. (2004). Briefly, Evercoat Everfix epoxy resin (Fibre Glass-Evercoat Co. Inc., Cincinnati, OH) with a black coloring is poured into Smooth-Cast® 385 molds created from *Mytilus californianus* shells. For each robomussel, a TidbiT logger (part #UTBI-001, Onset Computer Corporation, Mass.) is embedded in the polyester resin, which after hardening is smoothed and shaped to that of a real mussel using a Dremel tool. TidbiT loggers have an accuracy of ± 0.2°C over 0° to 50°C and a resolution 0.02°C at 25°C. The battery lasts for more than five years and the non-volatile memory stores approx. 42,000 12-bit temperature measurements, enough for more than 2.5 years with a sampling frequency of 30 min (which can be set from 1 second to 18 hours). Robomussels can be deployed in the field using A-788 Z-Spar Splash Zone Compound (Kop-Coat Inc, Pittsburgh, Pennsylvania, USA) to attach them to the rock or to any other substrata. Z-Spar sets in approximately 30 min and completely cures after a couple of hours (even underwater). TidbiT loggers are waterproof rated up to 300m, and thus no special care is needed to deal with immersion in seawater. Logger programming and data retrieval is done through the instruments' LEDs, which are exposed on the outside of the robomussel, using an USB optical communication cable and software from Onset Computer Corporation.

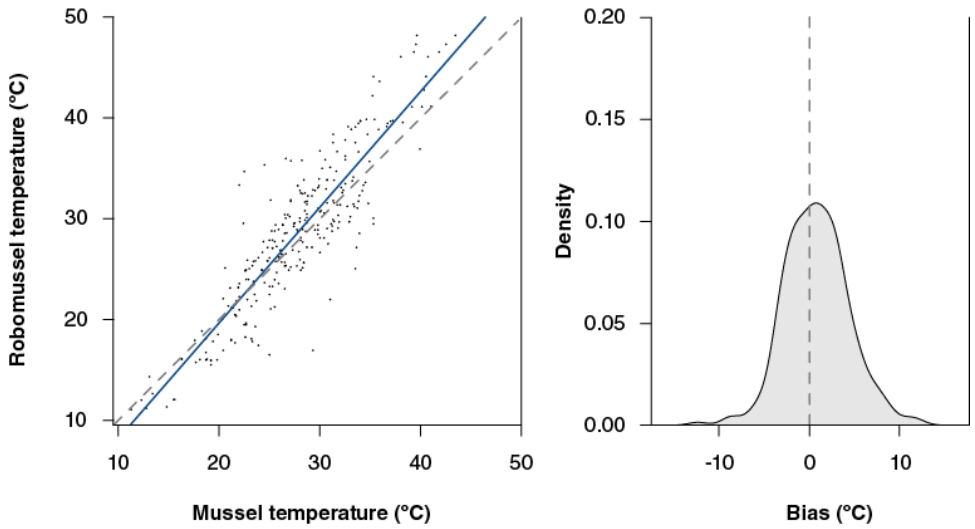

Fig. 2. Robomussel validation data (Root mean square error: 3.64 °C). Left: correlation between mussel body temperatures and robomussel measurements in a simulated mussel bed in the lab (276 pairs of measurements from 38 independent runs). The linear correlation (R= 0.89) is shown in blue and the reference dashed line y=x is depicted in gray. Right: Density plot of the differences (bias) between each robomussel measurement and the correspondent body temperature (mean bias: 0.82 °C).

Robomussel loggers have a thermal inertia comparable to that of a real mussel 74 mm in length. Under most field conditions, robomussels display temperatures within 1.5 – 2.0ºC of adjacent, living mussels (Helmuth & Hofmann, 2001). Notably, this compares very favorably to an unmodified Tibit logger, which displays an average error of 14°C to live mussels in the field (Fitzhenry et al. 2004). Fig. 2 shows some validation data acquired by comparing the body temperature of live mussels with robomussel measurements in a simulated mussel bed in the lab. In these conditions, loggers showed a linear correlation of 0.89, with a root mean square error of 3.64 ºC and a mean bias of 0.82 ºC.

One of the main shortcomings of the above described robomussels is a specific size size (~74 mm) where the specific heat × mass relationship crosses that of a real animal. Therefore, robomussels cannot be easily modified to mimic smaller animals, which in practice means that it is not possible to use this design to study other species of mussels such as *M. edulis*, *M. galloprovincialis* or *M. trossulus*. Also, the ability of robomussels to thermally match *M. californianus* seems to drop significantly when these loggers are used outside of a mussel bed (i.e., isolated robomussels do not perform as well as the others, B Helmuth, unpub. data). Finally, robomussels need to be entirely removed from the mussel bed each time they are serviced, which creates gaps and weakens the mussel bed. Nevertheless, data have shown that it is possible to obtain reasonably reliable results with the robomussel design, and that the errors in measurement are within the variability of what is recorded in the field within beds of a fixed substratum angle (Helmuth et al. 2006).

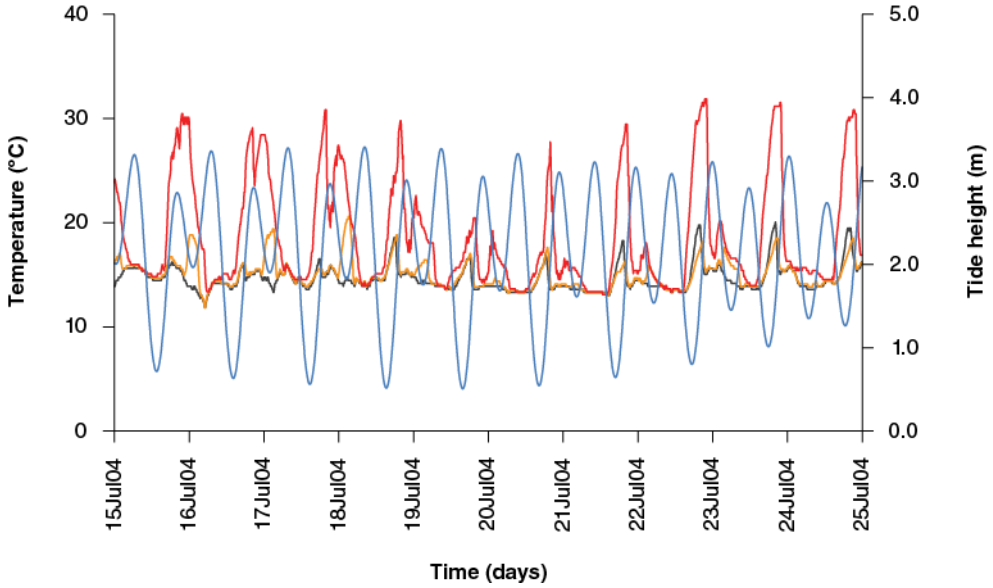

Fig. 3. Example of robomussel data from an exposed rocky shore in Seppings Island (SW Canada) taken between July 15th 2004 and July 25nd 2004. Times are in GMT. The black, orange and red lines show temperatures as measured by low-, mid- and high-intertidal loggers. Tidal heights are shown by the blue line.

Fig. 3 shows a 10-day long excerpt of the thermal profiles of three robomussels deployed in the low-, mid- and high- intertidal levels at a rocky shore in Seppings Island (Vancouver

Island, British Columbia, Canada). The cyclic effect of the tide is quite clear, with maximum body temperatures occurring during low tide and minimum daily temperatures coinciding with high tides (e.g., in July 16th, the second high-tide peak caused a sudden drop in the temperature of the high-intertidal robomussel). It is even possible to observe how the daily tidal oscillations interact with solar radiation, influencing body temperatures. For instance, in the beginning of the data series, low tides were occurring early in the morning and so all three loggers showed a short delay before starting to heat, while towards the end of the plot low tides were happening later in the day, and thus robomussels' temperatures started to increase earlier. Also evident is the difference in temperature caused by the tidal height at which loggers were deployed. For example, the low-intertidal logger never exceeds 20 ºC, while temperatures from the high-intertidal robomussel routinely reach 30 ºC.

Robolimpets can be built following the methodology described in Lima & Wethey (2009). Succinctly, these loggers consist of a lithium battery powering the circuit board from a DS1922L iButton (Dallas Semiconductor), embedded in a waterproof compound, inside an emptied real limpet shell (Fig. 4). Two exposed wires penetrating the shell serve as contacts for logger programming and subsequent data retrieval.

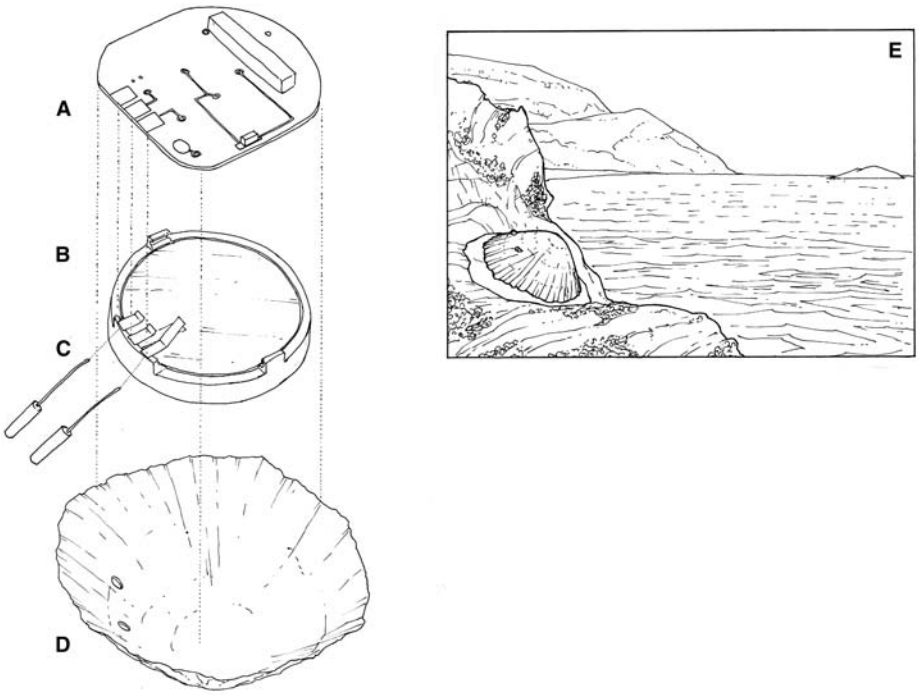

Fig. 4. Exploded view of the different parts used for building a temperature logger mimicking a *Patella* sp. (robolimpet). A: DS1922L iButton circuit board, B: DS1922L iButton battery, C: constantan wires (larger diameter) connected to wirewrap wires, D: *Patella* sp. shell with two holes to allow the constantan wires to protrude, E: representation of a robolimpet deployed in a rocky shore during low tide.

The DS1922 iButton hardware can be programmed to record up to 8192 readings at 0.5°C (enough for more than 5 months with a sampling frequency of 30 min) or 4096 readings at 0.0625°C resolution, measured at intervals from 1 s to 273 h, with an accuracy of ± 0.5°C. The first step in robolimpet assembly involves dissecting a DS1922L iButton. Using this procedure, even old, corroded iButtons can be recycled since the circuit board often remains perfectly functional despite deterioration of all other parts. iButtons have a stainless steel case that needs to be cut open with the help of a rotary tool fitted with an abrasive cutting wheel. For details on this procedure, see Lima & Wethey (2009). The circuit board is then separated from the battery clip and thoroughly washed with water and isopropanol if necessary. The original lithium battery (3V, 40 mAh) may be kept or may be replaced by a higher-capacity one (e.g., Panasonic BR1255-1VC). Two pieces of AWG 30 wirewrap wire (Digikey part K329-ND) are then soldered to the appropriate terminals, connecting the circuit board to the outside contacts in the shell. The external contacts are made of 1.6-mm-diameter non-corrodible constantan thermocouple wire (part EXPPT- 14, Omega Engineering), and are passed through holes previously drilled into the shell using a Dremel Rotary Tool fitted with a high-speed cutter (Dremel part 569). All electronic parts must be waterproofed to prevent corrosion. Thus, 3M Scotchcast 2130 Flame Retardant Compound is poured into shells previously fitted with the electronic parts and allowed to fully harden for at least 24 hours before deployment. This material has previously been shown to offer appropriate levels of waterproofing without compromising the match between temperature trajectories of live animals and temperature trajectories recorded by the loggers (Lima & Wethey, 2009).

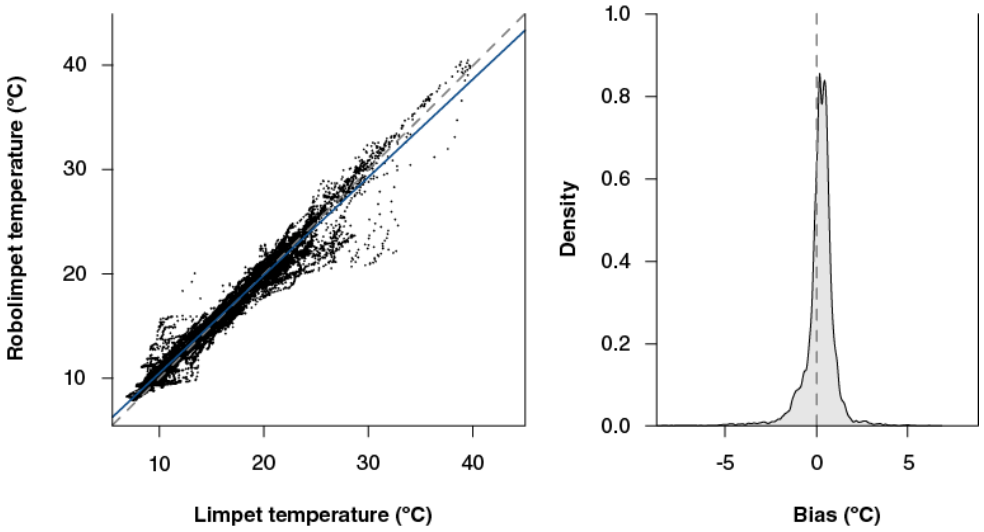

Fig. 5. Robolimpet validation data (Root mean square error: 0.94 °C). Left: correlation between limpet body temperatures and robolimpet measurements in the field (25,355 paired measurements from 5 replicates taken between May 26th 2008 and June 2nd 2008 at Friday Harbor, San Juan Island, Washington, USA). The linear correlation (R=0.98) is shown in blue and the reference dashed line y=x is depicted in gray. Right: Density plot of the differences (bias) between each robolimpet measurement and the correspondent body temperature (mean bias: 0.16 °C).

A connector cable can be made by stripping one end of a RJ-11 telephone cable and soldering two small alligator clips (Radio Shack, part 270-373) to the green and red wires (pins 3 and 4, respectively). These clips can then be connected to the robolimpet's negative and IO external contacts. The other end of the cable receives a RJ-11 telephone connector to be used with the 1-wire USB iButton adapter (Maxim IntegratedProducts part DS9490R - see Lima & Wethey (2009) for more details). Robolimpets can be programmed in the field with a laptop computer using free OneWireViewer software (www.maxim-ic.com). The alternative is to use a computer-independent, portable reader such as the NS-71 (Newshift Lda., Leiria, Portugal) to download data to a Secure Digital (SD) card.

Robolimpets have been shown to mach very tightly the temperature profiles of live animals in the field. Fig. 5 shows some validation data on the relation between body temperature on five live *Tectura persona* and the corresponding robolimpet measurements over more than a week, in a rocky shore in San Juan Islands, Washington. The two datasets have a linear correlation of 0.98, with a root mean square error of 0.94 ^{o}C and a mean bias of 0.16 ^{o}C, which is smaller than the variability observed between live animals separated by a couple of meters (Lima & Wethey, 2009). It is worth mentioning that these values were recorded by calibrated iButtons. Off-the-shelf iButtons are factory-calibrated, but since their calibration coefficients are stored in a volatile section of the memory and because it is very easy to momentarily disconnect de power from the circuit board while dehousing the electronics, calibration coefficients are often lost (this is obviously problematic when replacing the original battery). Calibration loss can be fixed by performing a 3-point calibration of the final assembled loggers under lab conditions. In this case, loggers are placed in a constant temperature chamber along with the probe of a precise thermocouple. The chamber is programmed to reach three specific temperatures (ideally, encompassing the full range of temperatures that robolimpets will likely experience in the field). Upon temperature stabilization, readings of the thermocouple (Ref_1, Ref_2, Ref_3) are compared with corresponding logs from the biomimetic sensors (Log_1, Log_2, Log_3), and for each measured temperature T in the field, a corrected T' can be derived as follows:

$$Dif_1 = Log_1 - Ref_1 \tag{1}$$

$$Dif_2 = Log_2 - Ref_2 \tag{2}$$

$$Dif_3 = Log_3 - Ref_3 \tag{3}$$

$$\alpha = (Dif_1 - Dif_3) + ((Dif_2 - Dif_1) \times (Ref_3 - Ref_1)/(Ref_2 - Ref_1)) \tag{4}$$

$$\beta = (Ref_3)^2 - (Ref_2 \times Ref_3) + (Ref_2 \times Ref_1) - (Ref_3 \times Ref_1) \tag{5}$$

$$c = -\alpha/\beta \tag{6}$$

$$b = (Dif_2 - Dif_1 - c \times ((Ref_2)^2 - (Ref_1)^2))/(Ref_2 - Ref_1) \tag{7}$$

$$a = Dif_1 - b \times Ref_1 - c \times (Ref_1)^2 \tag{8}$$

$$T' = T - a - (b \times T) - (c \times T^2) \tag{9}$$

Fig. 6 shows three examples of temperature profiles from robolimpets deployed for ten days in the low-, mid- and high-intertidal at a rocky shore in Biarritz (SW France). It is worth

noticing that during spring low tides (in the first part of the plot), all loggers reached similar high temperatures peaks (exceeding 32 ºC), irrespectively of their vertical position on the shore. On the other hand, during the neap tides (in the last days), the low-shore logger was spending relatively longer periods immersed in the sea and consequently never reached temperatures as high as those measured by the high-tide robolimpet. This clearly illustrates that even low-shore inhabiting limpets can reach potentially stressful temperatures during spring low tides, but that that the frequency of stressful events experienced by each individual is highly dependent on its vertical position on the shore.

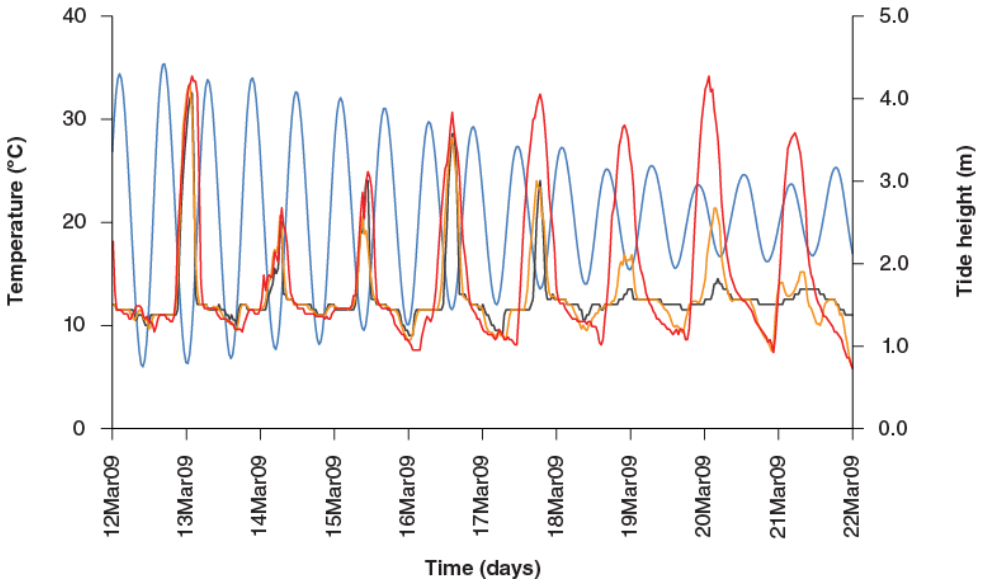

Fig. 6. Example of robolimpet data from an exposed rocky shore in Biarritz (SW France) taken between March 12th 2009 and March 22nd 2009. Times are in GMT. The black, orange and red lines show temperatures as measured by low-, mid- and high-intertidal loggers. Tidal heights are shown by the blue line.

In relation to their biomimetic characteristics, robolimpets outperformed robomussels in the sense that they not only show thermal profiles much closer to those displayed by live animals, but they also look more alike real animals (this is important because a higher mimetic capability makes them less likely to draw attention and thus less likely to be intentionally damaged). In addition, robolimpet electronics are much smaller and light-weighted (the dimensions of the coupled circuit board/battery do not exceed 14 × 4 mm, weighing approximately 1.5 g). This allows for a much higher flexibility in the logger design, which can be adapted to mimic different limpet species or even other gastropods, bivalves, barnacles, and other groups (see, for instance, robobarnacles and small robomussels in Lima & Wethey, 2009). Robolimpets are relatively inexpensive (each unit costs approximately 45 USD, substantially less than the cost of a robomussel, ~130 USD) and thus for roughly the same cost it is possible to deploy 3× more loggers covering a much larger geographical area. Finally, data downloading/servicing in the field is easier to do with these loggers.

Robolimpets have, however, some disadvantages over robomussels, namely a more complex and thus more time-consuming manufacturing process, and much smaller memory meaning that servicing must be done more frequently which may be problematic from the logistically and budgetary perspectives. Also, in robolimpets data are stored in a volatile section of the memory and thus are lost in the event of power failure. These loggers are also much more prone to leaking (at every six months, approximately one fourth of the loggers are lost), which can also be limiting when performing large-scale studies.
In sum, sensors/loggers mimicking the thermal characteristics of sessile intertidal species offer the opportunity to obtain data series with thousands of body temperatures along a wide range of microhabitats. Equally important is the ability to measure environments where these organisms do not occur, which may be extremely informative to understand the biogeographic patterns or the physiological requirements of a given species (Wethey, 2002; Lima et al., 2006).Taking measurements of body temperatures in areas where a given species does not occur is obviously problematic. The biomimetic loggers here described are a relatively easy way to overcome this problem and still measure temperatures that closely resemble those experienced by real organisms. They potentially allow building large-scale networks of sensors, obtaining fundamental data for ecological, physiological, biogeographical or even climate monitoring studies.
New advances are being made in these technologies, including a version of the robomussel that uses RFID technology to transmit data, thus eliminating the need to remove loggers after each deployment. By using materials with a higher mass and/or specific heat capacity, it will also be possible to manufacture smaller versions of the instrument to mimic smaller congeners (~50mm).

4. Biomimetic desiccation data loggers

The dehydration, or desiccation, tolerances of an organism depend on the physiological response, whether it is the production of stress proteins (Benoit et al., 2010; Mizrahi et al., 2010) or change in energy metabolism (Churchill & Storey, 1995; Santini, et al., 2001). These tolerances dictate how long an organism can survive without replenishing its water content, thus determining suitable habitat as a function of distance from a water source and also outlining appropriate organismal behavior. However, habitat cannot be generalized only by its proximity from water. Regardless of an organism's ability to combat or tolerate water loss, the severity of the desiccation it faces in any habitat is also dependent on meteorological factors. Air temperature, ambient humidity, substrate properties, and wind all affect evaporative water loss. In the intertidal zone, organisms face a choice of microclimates that can be restricted by vertical tidal height, maximizing feeding time (Borrero, 1987; Schneider et al., 2010), minimizing time vulnerable to predators and minimizing exposure to abiotic stresses (Petes et al., 2008; Smee et al., 2010).
The biomimetic desiccation data loggers - BDDL (also known as desiccation robolimpets) described in this section are designed to serve as a relative measure of potential desiccation stress that intertidal limpets are exposed to in a particular microclimate. The functional unit of each BDDL is a DS1923 Hygrochon iButton (Dallas Semiconductor) with simultaneous relative humidity (RH) and temperature measuring capabilities. Thus, the sensors in these BDDL can record a relative measure of the change in water content of the soft tissue, as well as body temperature of the modeled organisms. Each DS1923 iButton was dissected, modified, and encased in a limpet shell following the general methodology used for the production of robolimpets (Lima & Wethey, 2009, see also previous section).

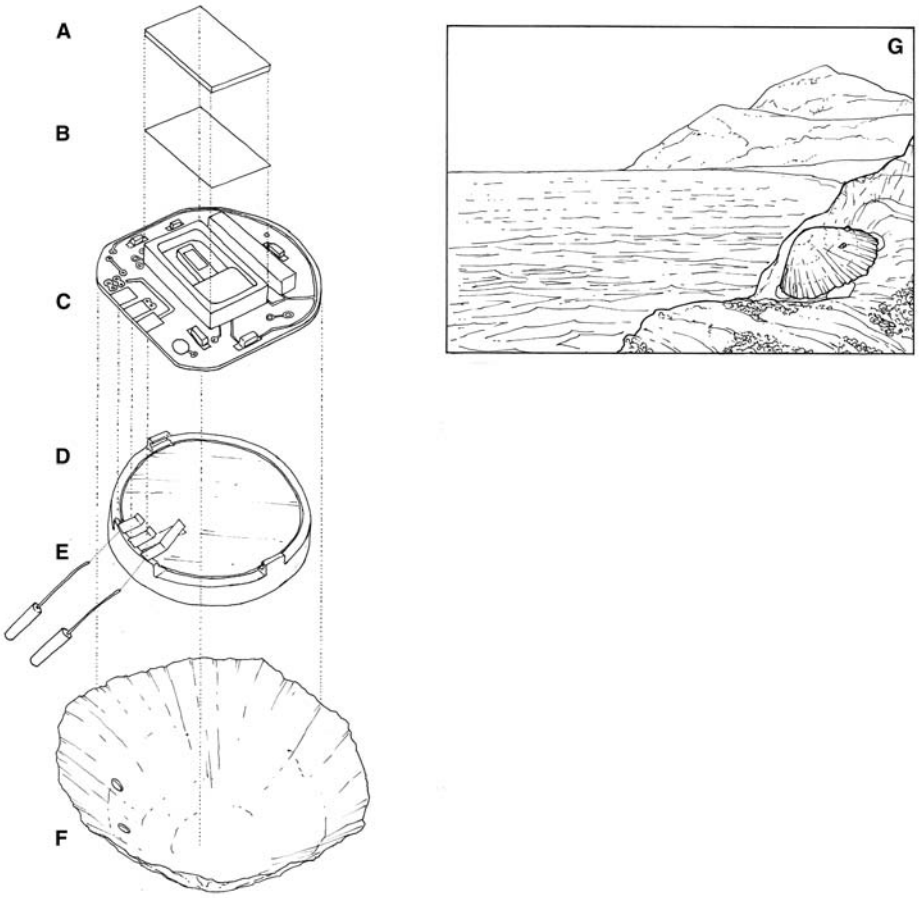

Fig. 7. Humidity logger mimicking a *Patella* sp. A: viscose pad, B: Tyvek polyethylene fiber paper, C: DS1923 iButton circuit board, D: DS1923 iButton battery, E: constantan wires (larger diameter) connected to wirewrap wires. F: *Patella* sp. shell with two holes to allow the constantan wires to protrude, G: Representation of a humidity sensor deployed in a rocky shore during low tide.

The RH sensor of the DS1923 iButtons is a structurally delicate thermoset polymer capacitive sensing element (Pan et al., 2010) and therefore must be protected from physical abrasions, which was done by covering it with a single layer of Tyvek polyethylene fiber paper (DuPont, Wilmington, DE) adhered with super glue control gel (Loctite, Westlake, OH) around the edge of the humidity sensor casing. Tyvek polyethylene fiber paper is a tough, durable and tear-resistant material unaffected by contact with liquid water but permeable to water vapor. The coupled electronic circuit/battery from the DS1923 was encased in the limpet shell with the RH sensor on the ventral face (where the limpet would normally contact the substrate, see Fig. 7) and all the electronic parts waterproofed with 3M Scotchcast 2130 Flame Retardant Compound. Caution was taken to prevent the Tyvek and

RH sensor from being covered by the potting compound, facilitating the diffusion of ambient water vapor into the RH sensor. To mimic water-saturated soft tissues of the live organisms, a 1 × 1 cm piece of viscose (Boat Towl, Paddling.net, Caledonia, MI), a non-biodegradable, highly absorptive fabric, was placed over the face of the humidity sensor and the cloth glued around its edges to the set Scotchcast Compound. Prior to sampling this fabric was saturated with freshwater and the evaporation of the water was monitored with the RH sensor. This design allows meteorological events (e.g., wind, solar radiation) to act on the soft tissue mimic just as those factors would act on the body of real limpets, and be measured by the RH sensor.

In contrast to temperature robolimpets, desiccation loggers cannot be completely attached to the substrate surface because that would prevent water vapor transfer between the ventral face of the biomimetic logger and the surrounding environment. Desiccation loggers were therefore temporarily attached to the rocky surfaces using small amounts of modeling clay placed on the edge of the shell, leaving enough small gaps for water vapor exchange (Fig. 7 G).

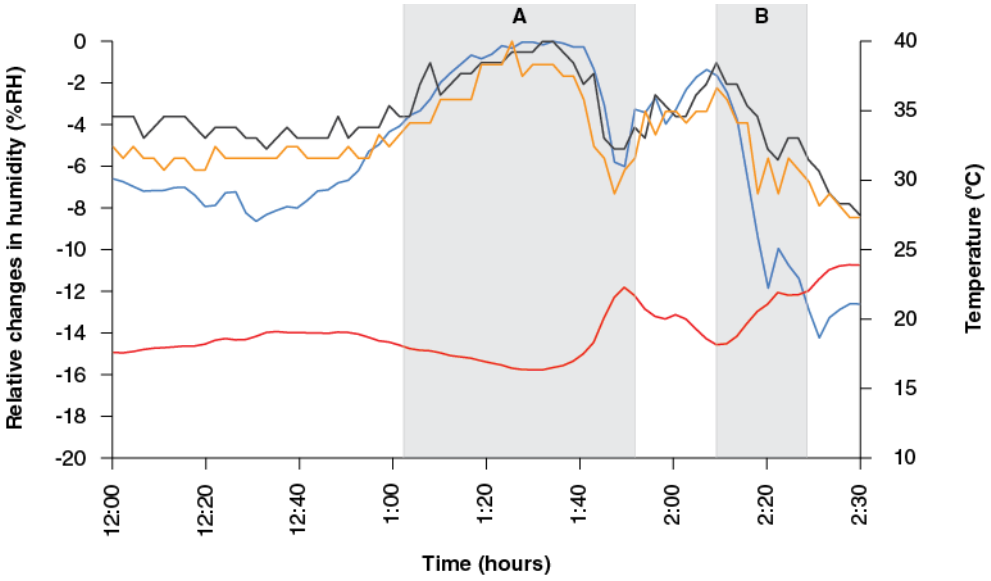

Fig. 8. Comparison between water loss measured in a live limpet (*Patella vulgata* - black line) and water loss as recorded by two biomimetic desiccation loggers (blue and orange lines) on a mid-intertidal crevice on a rocky shore at Le Croisic (NW France) on June 14th 2010. The temperature trajectory of the robolimpet is shown in red. A 45-minute rain storm occurred during period A, followed by sun at period B.

The described BDDL were compared against live limpet desiccation rates, measured in vivo via relative humidity monitoring of the mantle cavity. Neither the BDDL nor the in vivo measurements provide a direct estimate of the quantity of water lost due to evaporation. Rather, the sensor and the live animals behave like "a wet sponge that can lose some water but remain wet." As expected, both live limpets and the BDDL have fully saturated (100% RH) internal humidity when shaded or when there is no wind. However, abrupt peaks in humidity were recorded during deployments and were associated with the local weather

conditions, such as gusts of wind, sun radiation or precipitation (Figs. 8 and 9). It is important to note that these changes were synchronous between each BDDL and its respective live limpet measurement. Gradual, longer lasting changes in the recorded humidity of live limpets and BDDL were indicative of precipitation (Figs. 8) and the presence of solar radiation (Fig. 9), both of which could be dually verified by changes in the body temperature. In fact, during the field deployment at Le Croisic (SW France), changes in RH were inversely correlated with changes in body temperature (Fig. 8).

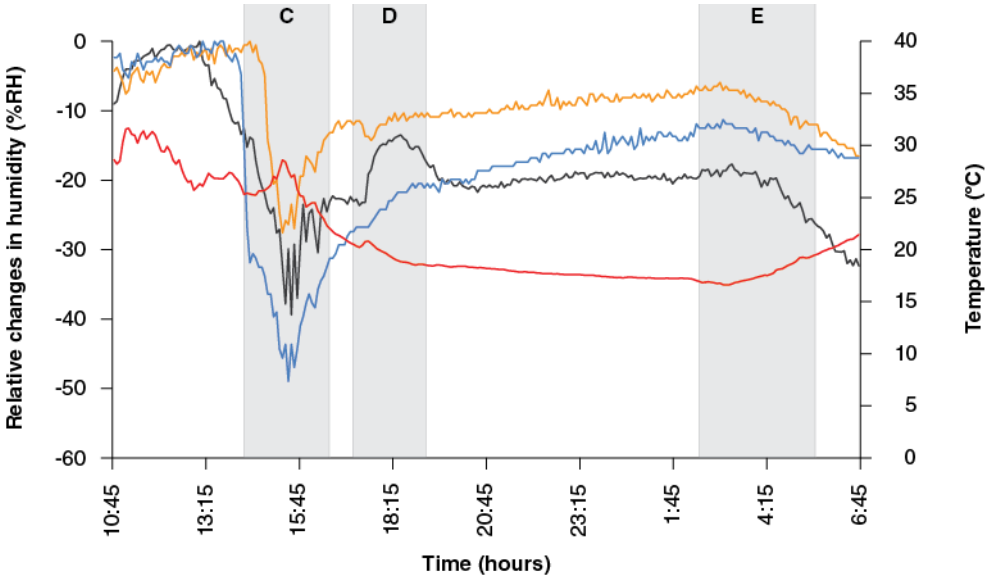

Fig. 9. Comparison between water loss measured in a live limpet (*Patella vulgata* - black line) and water loss as recorded by two biomimetic desiccation loggers (blue and orange lines) on a supralitoral rocky surface at Lavra (NW Portugal) on June 23rd-24th 2010. The temperature trajectory of the limpet is shown in red. Period C corresponds to strong afternoon sun, which was followed by sunset at D. Temperatures decreased gradually during the night, but rose at sunrise (E), causing evaporative water loss in the live animal and in the biomimetic loggers.

On the most basic level, BDDL can measure the frequency and relative magnitude of desiccation stress associated with wind and larger meteorological events as experienced by the study organism, in any possible microclimate. Wind, in combination with low humidity, has been suggested as a dominant physical stressor on some rocky shores (Bertness et al., 2006; Bazterrica et al., 2007). The scope of quantifiable parameters is limited in this data logger, allowing several options for interpretation. A catalogue of the data loggers' behaviors referenced against real meteorological events, specific to any study site, can easily be compiled, allowing for a more accurate interpretation of data. The electronic basis of BDDL also presents an obstacle for long term and widespread field monitoring. The humidity sensor acts a gateway for salt to enter the electronics of the DS1923 iButton and thus salt water corrosion of the device is inevitable for long term field monitoring. The RH sensor has an accuracy of ± 3.5 % RH, but according to the manufacturer (Honeywell -

http://sensing.honeywell.com), a repeated exposure of the RH sensor to high humidity environments can cause a reversible 3% shift in the measurements. The DS1923 iButton also costs approximately 85 USD, making each data logger relatively expensive, especially when considering its susceptibility to corrosion and anticipated short field life.
Employing BDDL in the study of intertidal ecology and climate change can provide insights into the importance of protection from desiccating physical stress for a specific organism. This tool, in combination with other biomimetic data loggers mentioned in this chapter, can provide a more refined representation of the effects of microclimate in the physical stress of organisms, a key to understand and forecast how long-term global climate change can influence the biogeography and ecology of intertidal species worldwide.

5. Biomimetic wave force data loggers

Disturbance by wave forces is a major factor influencing the distribution, abundance, activities and temporal dynamics of intertidal organisms. Such forces cause erosion of individuals, create patches of bare space, set limits to body size, and limit the foraging abilities of consumers (Lewis, 1964; Dayton, 1971; Koehl, 1976; Menge, 1976; Sousa, 1979; Paine & Levin, 1981; Denny et al., 1985; Denny, 1995; Gaylord, 2000; Wethey, 2002; Denny et al., 2003; Carrington et al., 2009).
From the point of view of an organism in the shore, it is the total force which determines its ability to resist erosion, so direct measurements of both lift and drag components of force are essential for predicting survival or death. Still, there is relatively poor quantitative knowledge of these forces on the spatial and temporal scales over which they operate. Maximum forces have been estimated with spring-scale dynamometers since the 1970's (Jones & Demetropoulos, 1968; Denny, et al., 1985; Denny, et al., 2003; Helmuth & Denny, 2003), but these measure maxima over time scales of days to weeks. Instantaneous forces on one or more axes have been measured on models of organisms (Denny, 1982; Denny, 1995), or live organisms (Boller & Carrington, 2006) but these have been limited to short deployments. A common approach has been to estimate or measure water velocities at the substratum and use equations for drag and lift to predict the forces that should have occurred during those conditions (Denny, et al., 1985; Denny, 1995; Denny & Wethey, 2000; Gaylord, 2000), but the extent to which the theoretical estimates of wave forces and wave heights actually represent conditions experienced by organisms in the surf zone is not known (e.g., Helmuth & Denny, 2003). Also, because big waves and correspondingly big forces are rare and difficult to measure, most authors calculate from probability distributions the maximum forces that organisms would likely experience in a year, rather than actually measuring them (e.g., Denny, et al., 1985; Denny, 1995).
Therefore there is a clear need for instruments that would make continuous direct measurements of drag and lift forces, wave heights, and their rates of change, over a wide range of habitats, organisms, and hydrodynamic conditions from calm to extreme storms. Such instruments should be relatively cheap, and be capable of long-term deployments in the field. Here, we describe a three-axis force sensor designed to measure wave forces and wave heights on a time and size scale appropriate for organisms inhabiting the surf zone of rocky intertidal shores. The instrument is capable of continuous deployments of several months duration. The sensor/logger package consists of a three axis force transducer connected to a resin model of a mussel (*Mytilus edulis*), a custom-made data logger in a waterproof housing and respective communication cables (Fig. 10).

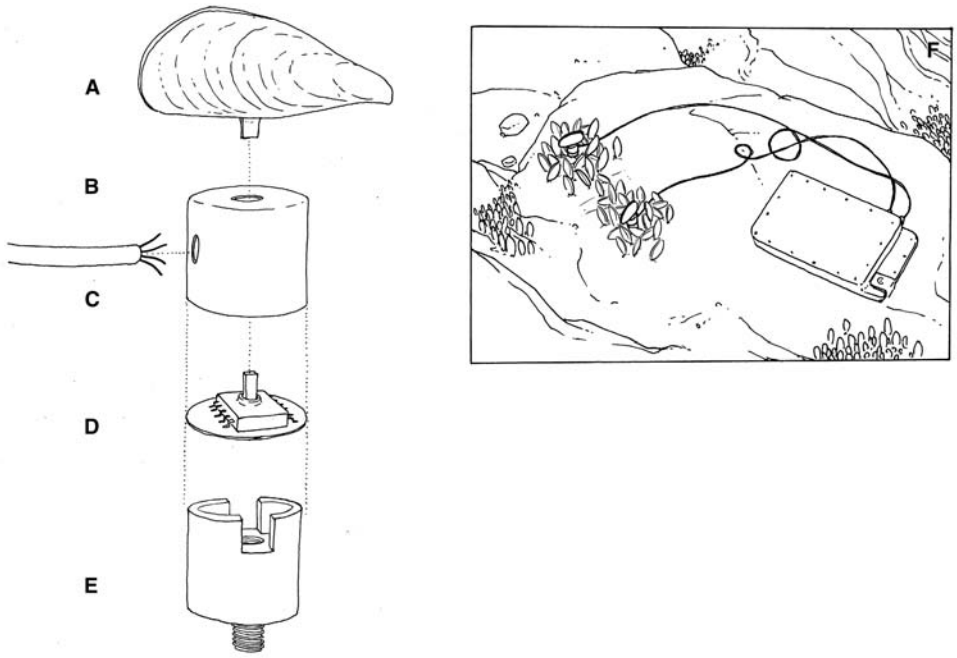

Fig. 10. Wave force logger mimicking a *Mytilus edulis*. A: polyester mussel model, B: copper pipe cap, C: sensor cable, D: printed circuit board with "SurfStick" sensor, E: polycarbonate plug with threaded rod for attachment. F: two wave force loggers deployed in musselbeds in the rocky intertidal together with an aluminum housing protecting the data logger.

The three axis force transducer was based on the CTS Corp Series 109 SurfStik (CTS Corp, Berne, Indiana, USA), a surface mount device with four strain gauges arranged around a 1.78 mm square ceramic post designed for use as the pointing device in notebook computer keyboards (Fig 10 D). These devices are rated to withstand forces of 200N and 40N in the vertical and horizontal directions, respectively. The SurfStick was soldered to a small circular printed circuit board, and embedded with epoxy within a standard copper cap for ½" (12.7 mm) ID copper water pipe, with the ceramic post protruding through a hole in the center of the flat face of the cap. A shielded signal cable was passed through a hole in the side of the cap. The base of the copper cap was sealed by a polycarbonate plastic plug including a slot for the cable, and a threaded hole on the exposed side.

A polyester resin model of a blue mussel *Mytilus edulis* was molded with a square brass tube protruding from the ventral surface where byssal threads emerge from the shell of a live animal (Fig. 10 A). The brass tube was fitted over the ceramic post of the force sensor and secured with Devcon 2-ton epoxy (Devcon Corp, Danvers, Massachusetts, USA). The sensor was calibrated by hanging weights from the top edge of the shell in orientations parallel and perpendicular to the ceramic post.

The strain gauges were arranged in 3 Wheatstone bridge circuits (Fig. 11), so that 3-axis forces could be measured. For x-axis forces, the east and west resistors were arranged as one

half of a bridge, sensed from a connection between E and W. For y-axis forces, the north and south resistors were placed in a half-bridge, sensed from a connection between N and S. The other half of these bridges were pairs of 10 KΩ 1% metal film resistors on opposite sides of an 11-turn cermet 100 Ω potentiometer (Fig 11, "trm_x, trm_y"). The zero point for each sensor was adjusted with the potentiometer. The z-axis measurement used all four strain gauges together configured as a single arm of another Wheatstone bridge. The other arms of the z bridge were 10 KΩ 1% metal film resistors, and an 11-turn cermet 100 Ω potentiometer was used to set the zero (Fig 11, "trm_z"). The bridges were excited with a precision voltage reference (Burr Brown INA125), and the signals were amplified by Burr Brown INA125 and INA2126 instrumentation amplifiers. The circuit (Fig. 11) was produced on a two-layer printed circuit card (ExpressPCB Corp, Santa Barbara, California, USA).

Water depth was measured with a stainless steel absolute pressure sensor (Sensym ICT Series19, 30 psi), excited and amplified by a Burr Brown INA125 instrumentation amplifier. The pressure sensor was mounted in the instrument housing.

Analog signals were digitized at 40 Hz and recorded using a Persistor CF2 (Persistor Instruments, Bourne, Massachusetts, USA) microprocessor-based data logger, with a Burr-Brown 16-bit analog to digital converter (ADS8344, on a Persistor R216 "recipe card"). Data were stored on 2GB compact flash cards (as used in digital cameras). The data logger is 5 cm x 7.5 cm, and the analog amplifier card is a similar size. In order to reduce power drain, the CF2 microprocessor (Motorola 68332) is run at 4 MHz, and awakened from sleep-mode by a programmable interrupt timer running at 40 Hz for data acquisition. The system draws approximately 5 mA and is powered with three 3V lithium C-cells (5 ampere-hour), enough for deployments up to 90 days. The ability to make continuous measurement for several months is a great advantage over similar force loggers which are limited to less than 1-hour deployments by data storage capacity (Boller & Carrington, 2006).

Analog and digital electronics boards and power supplies were mounted in a low profile aluminum housing (5 cm x 23 cm x 15 cm, including 1.3cm thick lid and 1.6 cm thick base). The sensor cable was attached to the housing with waterproof 4-pin connectors (Type 9104.14 and 9104.54, Ikelite Corp, Indianapolis, Indiana, USA). The instrument package was designed to withstand impact from wave-borne rocks, and to resist drag and lift forces. It was attached to the rock by six 6.35 mm diameter stainless steel wedge anchors placed in holes drilled in the rock. The electronics package was attached approximately 0.5 m away from the sensor so that it would not disrupt fluid flow around the sensor to any greater extent than the variable topography in the intertidal zone. A sacrificial zinc anode was attached to the housing to prevent corrosion. In SW England, five housings were experimentally deployed in the surf zone of exposed to moderately exposed rocky shores for a total of 120 housing-days with no damage or failures. Wave heights on top of the housings ranged from 0.5m to 3m during the deployments.

The sensor was attached to the rock by drilling a ¾" diameter hole in the rock within a patch of mussels, filling the hole with Z-Spar Splash Zone Compound (Kop-Coat Inc, Pittsburgh, Pennsylvania, USA), screwing a 1 cm length of threaded rod into the base of the sensor, and pressing the threaded rod and base of the sensor cap into the Z-Spar until the mussel model was level with the height of the surrounding mussel bed. The cable was anchored to the rock with cable ties attached to stainless steel wedge anchors. During the deployment period, only 1 mussel sensor broke after being hit by a wave-borne object.

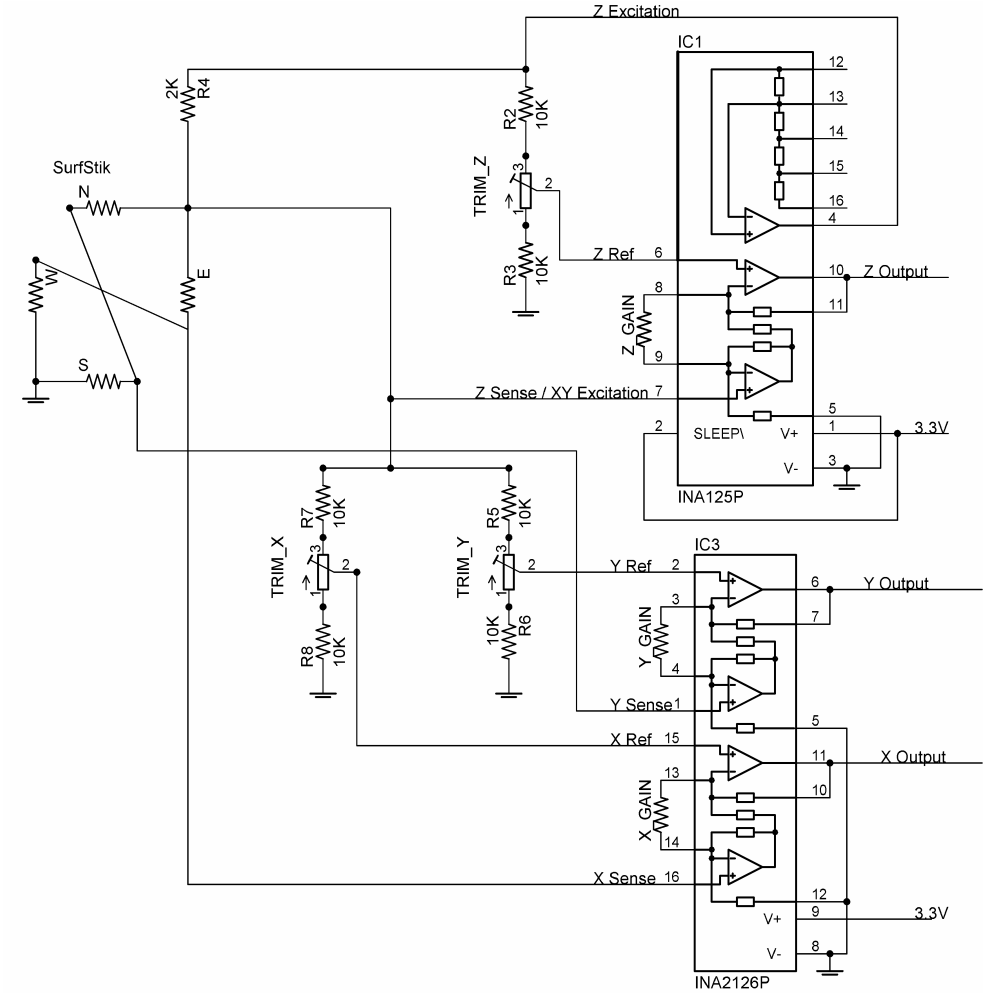

Fig. 11. Schematic Diagram of force sensor circuit. On the left hand side of the circuit is the CTS "SurfStik", with strain gauge resistors on the four sides (N,S,E,W) of the ceramic post.

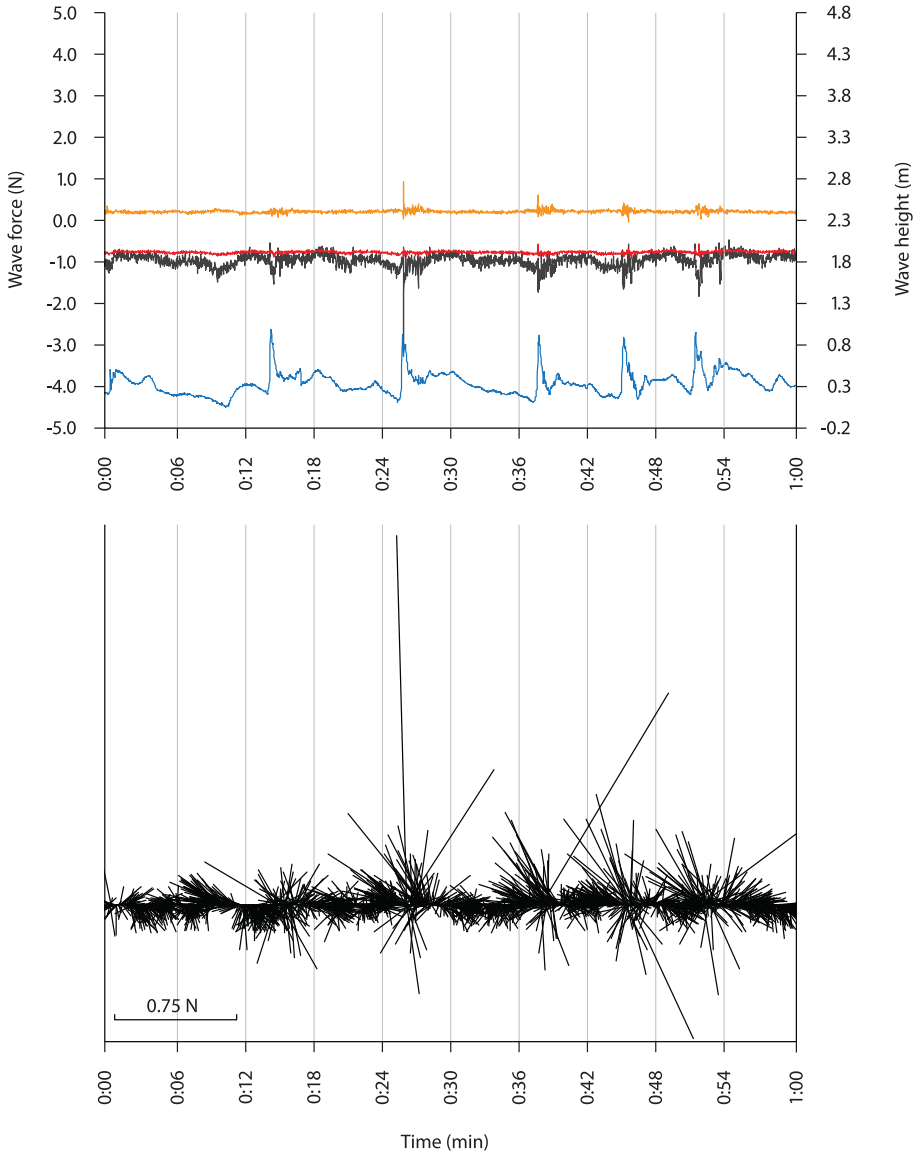

Fig. 12. Data from a mussel-shaped wave force sensor, acquired on an exposed rocky shore in Lansallos (SW England) in February 19th 2003. Top Panel: three axis force record and wave height during a 1 minute period. Red = x, orange=y, black=z (scale on left in newtons), blue= wave height (scale on right, in meters). Lift forces are displayed as negative on the force axis. Note that drag forces (red and orange) are smaller than lift forces, and that not all waves of equivalent height generate equivalent forces. Bottom Panel: vector plot of horizontal forces during the same 1 minute period. Note the rotational motion as waves cross the sensor.

The system has an effective resolution of 0.1N in the vertical direction and 0.05N in the horizontal, taking into account electrical noise. The maximum forces recorded were 55N impact (downward), 8N lift (upward), and 4N drag (horizontal). In order to detect the forces on a wave-by wave basis, a zero crossing detector was used to find the beginning and end of each wave in 1 min sections of the data stream. The maximum and minimum water heights in each wave were used to determine wave height. The maximum force along all three axes results from highly complex interactions between animals and waves in the surf zone. Of particular note, lift forces tended to be 3 to 4 times larger than drag forces because the sensor was deployed within mussel beds, where individuals are sheltered from drag by their neighbors.

Lift forces are significant in this circumstance because skimming flow of water moves rapidly over the surface of the bed, and water is stagnant at the bottom of the bed. The velocity difference between the top and the bottom of the bed is presumably responsible for generating lift. This result is consistent with the Pitot-tube observations of Denny (1987) on the pressure differences between the top and bottom of a mussel bed during flow. From the point of view of mussels compacted in extensive beds, therefore, lift is far more important than drag. Drag forces are probably important only for exposed individuals located outside from the mussel bed.

Water velocities and accelerations were large when waves crossed over the sensor package (Fig. 12). In the figure, a 0.75 m wave had a vertical water velocity of 13 m s^{-1}, and a vertical acceleration of 300 - 500 ms^{-2}, all associated with flow reversals and acceleration reversals within less than a second. These directly measured values are similar to those calculated from surf-zone force records by Denny et al., (1985). In larger waves, accelerations on the order of 1000 ms^{-2} were observed.

Not all waves of the same size and shape generate the same magnitude of forces on individuals. Thus two waves can be of the same size, and generate forces that differ by a factor of 5 or 10 (fig. 12). The reason for this is that the mussel is in a fixed location, so it is sensing the environment in an Eulerian manner. Hence, the exact size and trajectory of each wave determines how it will react with an individual point on the bottom. Waves with slightly different trajectories will sweep specific locations on the bottom with different velocities, creating different forces on the animal or sensor. The average of a large number of waves will be similar to the expected value of force or velocity, but the individual wave may generate much larger or much smaller forces. These results and those of Gaylord (1999; 2000) and Helmuth & Denny (2003) indicate that there is a strongly probabilistic relationship between wave height and water velocity or wave force. For instance, among waves of height 0.5 m to 0.6 m, the 50th median value of water velocity was 2.59 ms^{-1}, whereas the 90th, 95th, and 99th percentiles of velocity were 3.98, 4.49, and 5.66 ms^{-1}, respectively. Thus, calculations of average conditions or the use of regressions of wave height to velocity will estimate the conditions experienced only in the median wave in the overall distribution, and will underestimate the larger velocities and forces in half of the waves experienced by organisms in the surf zone. These velocities in the upper half of the distribution can be 2 to 5 times greater than the median, and therefore forces that scale with the square of velocity can be 4 to 25 times greater than the median. These data reinforce the idea that it is necessary to have reliable measurements of the distributions of forces generated by waves in order to be able to fully understand their influence on intertidal communities.

The described biomimetic wave force data logger provides an inexpensive method for directly measuring the distributions of lift and drag forces, wave heights, vertical water

velocities and accelerations on time and spatial scales appropriate for studies of the effects of disturbance on intertidal communities. This sensor system can be adapted to study the effect of waves on other sedentary intertidal organisms, by changing the geometry of the sensor head to mimic barnacles, gastropods, algae, and other groups. Because it measures wave height simultaneously with forces, it avoids the tenuous link between offshore measurements of waves, and extrapolation via theory to the environment of the surf zone.

6. Acknowledgements

All drawings by André L. Araújo. The authors would also like to thank Jerry Hilbish, Nuno Queiroz and Rui Seabra for their help during fieldwork and for their insightful suggestions that often resulted in design improvements. Funding was provided by NOAA (NA04NOS4780264), NASA (NNG04GE43G and NNX07AF20G), National Science Foundation (IBN 0131308) and Fundação para a Ciência e a Tecnologia - FCT (PTDC/MAR/099391/2008 and SFRH/BPD/34932/2007) grants, and a University of South Carolina Residential Mini-Grant. Brian Bittner of CTS Corp provided evaluation samples of the SurfStik. Arthur Illingworth and Allen Frye designed and built the waterproof housings for the wave sensors.

7. References

Bazterrica, M. C.; Silliman, B. R.; Hidalgo, F. J.; Crain, C. M. & Bertness, M. D. (2007). Limpet grazing on a physically stressful Patagonian rocky shore, *Journal of Experimental Marine Biology and Ecology,* 353, 1, 22-34, 0022-0981

Benoit, J. B.; Lopez-Martinez, G.; Phillips, Z. P.; Patrick, K. R. & Denlinger, D. L. (2010). Heat shock proteins contribute to mosquito dehydration tolerance, *Journal of Insect Physiology,* 56, 2, 151-156, 0022-1910

Berke, S. K.; Mahon, A. R.; Lima, F. P.; Halanych, K. M.; Wethey, D. S. & Woodin, S. A. (2010). Range shifts and species diversity in marine ecosystem engineers: patterns and predictions for European sedimentary habitats, *Global Ecology and Biogeography,* 19, 2, 223–232, 1466-8238

Bertness, M. D.; Crain, C. M.; Silliman, B. R.; Bazterrica, M. C.; Reyna, M. V.; Hildago, F. & Farina, J. K. (2006). The community structure of Western Atlantic Patagonian rocky shores, *Ecological Monographs,* 76, 3, 439-460, 0012-9615

Boller, M. L. & Carrington, E. (2006). In situ measurements of hydrodynamic forces imposed on Chondrus crispus Stackhouse, *Journal of Experimental Marine Biology and Ecology,* 337, 2, 159-170, 0022-0981

Borrero, F. J. (1987). Tidal height and gametogenisis: reproductive variation among populations of *Geukensia demissa*, *Biology Bulletin,* 173, 1, 160-168, 0006-3185

Broekhuysen, G. J. (1941). A preliminary investigation of the importance of desiccation, temperature and salinity as factors controlling the vertical distribution of certain intertidal marine gastropods in False Bay, South Africa, *Transactions of the Royal Society of South Africa,* 28, 255–292, 0035-919X

Carrington, E.; Moeser, G. M.; Dimond, J.; Mello, J. J. & Boller, M. L. (2009). Seasonal disturbance to mussel beds: Field test of a mechanistic model predicting wave dislodgment, *Limnology and Oceanography,* 54, 3, 978–986, 0024-3590

Churchill, T. & Storey, K. (1995). Metabolic effects of dehydration on an aquatic frog, *Rana pipiens*, *Journal of Experimental Biology,* 198, 1, 147-154, 0022-0949

Connell, J. H. (1961a). Effects of competition, predation by *Thais lapillus*, and other factors on natural populations of the barnacle *Balanus balanoides*, *Ecological Monographs,* 31, 61–104, 0012-9615

Connell, J. H. (1961b). The influence of intra–specific competition and other factors on the distribution of the barnacle *Chthamalus stellatus*, *Ecology,* 42, 4, 710–723, 0012-9658

Connell, J. H. (1972). Community interactions on marine rocky intertidal shores, *Annual Review of Ecology and Systematics,* 3, 169-192, 0066-4162

Crisp, D. J., Ed. (1964). The effects of the severe winter of 1962-63 on marine life in Britain, *Journal of Animal Ecology,* 33, 179-210, 0021-8790

Dahlhoff, E. P. (2004). Biochemical Indicators of Stress and Metabolism: Applications for Marine Ecological Studies, *Annual Review of Physiology,* 66, 1, 183-207, 0066-4278

Dayton, P. K. (1971). Competition, disturbance and community organization: the provision and subsequent utilization of space in a rocky intertidal community, *Ecological Monographs,* 41, 4, 357–389, 0012-9615

Denny, M. (1995). Predicting Physical Disturbance: Mechanistic Approaches to the Study of Survivorship on Wave-Swept Shores, *Ecological Monographs,* 65, 4, 371-418, 0012-9615

Denny, M.; Daniel, T. & Koehl, M. (1985). Mechanical limits to size in wave-swept organisms, *Ecological Monographs,* 55, 69-102, 0012-9615

Denny, M. W. (1982). Forces on intertidal organisms due to breaking ocean waves: design and application of a telemetry system, *Limnology and Oceanography,* 27, 178–183, 0024-3590

Denny, M. W. (1987). Lift as a mechanism of patch initiation in mussel beds, *Journal of Experimental Marine Biology and Ecology,* 113, 3, 231-245, 0022-0981

Denny, M. W.; Miller, L. P. & Harley, C. D. G. (2006). Thermal stress on intertidal limpets: long-term hindcasts and lethal limits, *The Journal of Experimental Biology,* 209, 2420-2431, 0022-0949

Denny, M. W.; Miller, L. P.; Stokes, M. D.; Hunt, L. J. H. & Helmuth., B. S. T. (2003). Extreme water velocities: Topographical amplification of wave-induced flow in the surf zone of rocky shores, *Limnology and Oceanography,* 48, 1-8, 0024-3590

Denny, M. W. & Wethey, D. S. (2000). Physical processes that generate patterns in marine communities, In: *Marine Community Ecology*, M. Bertness; S. Gaines & M. Hay, (Ed), 1-37, Sinauer Associates, Sunderland, Massachusetts

Firth, L. B. & Williams, G. A. (2009). The influence of multiple environmental stressors on the limpet *Cellana toreuma* during the summer monsoon season in Hong Kong, *Journal of Experimental Marine Biology and Ecology,* 375, 1-2, 70-75, 0022-0981

Fitzhenry, T.; Halpin, P. M. & Helmuth, B. (2004). Testing the effects of wave exposure, site, and behavior on intertidal mussel body temperatures: Applications and limits of temperature logger design, *Marine Biology,* 145, 2, 339-349, 0025-3162

Foster, B. A. (1971). Desiccation as a factor in the intertidal zonation of barnacles, *Marine Biology,* 8, 12–29, 0025-3162

Gaylord, B. (1999). Detailing agents of physical disturbance: wave-induced velocities and accelerations on a rocky shore, *Journal of Experimental Marine Biology and Ecology,* 239, 1, 85-124, 0022-0981

Gaylord, B. (2000). Biological Implications of Surf-Zone Flow Complexity, *Limnology and Oceanography,* 45, 1, 174-188, 0024-3590

Gilman, S. E.; Wethey, D. S. & Helmuth, B. (2006). Variation in the sensitivity of organismal body temperature to climate change over local and geographic scales, *Proceedings of the National Academy of Sciences,* 103, 25, 9560–9565, 1091-6490

Harley, C. (2008). Tidal dynamics, topographic orientation, and temperature-mediated mass mortalities on rocky shores, *Marine Ecology Progress Series,* 371, 37-46, 0171-8630

Harley, C. D. G. & Helmuth, B. S. T. (2003). Local- and regional-scale effects of wave exposure, thermal stress, and absolute versus effective shore level on patterns of intertidal zonation, *Limnology and Oceanography,* 48, 4, 1498–1508, 0024-3590

Hawkins, S. J.; Hartnoll, R. G.; Kain, J. M. & Norton, T. A. (1992). Plant-animal interactions on hard substrata in the North-east Atlantic, In: *Plant–Animal Interactions in the Marine Benthos*, D. John; S. J. Hawkins & J. Price, (Ed), 1–32, Clarendon Press, 0-19-857754-O, Oxford

Helmuth, B. (1998). Intertidal Mussel Microclimates: Predicting the Body Temperature of a Sessile Invertebrate, *Ecological Monographs,* 68, 29-52, 0012-9615

Helmuth, B. (1999). Thermal biology of rocky intertidal mussels: Quantifying body temperatures using climatological data, *Ecology,* 80, 1, 15–34, 0012-9658

Helmuth, B. (2002). How do we measure the environment? Linking intertidal thermal physiology and ecology through biophysics, *Integrative and Comparative Biology,* 42, 4, 837-845, 1540-7063

Helmuth, B.; Broitman, B. R.; Yamane, L.; Gilman, S. E.; Mach, K.; Mislan, K. A. S. & Denny, M. W. (2010). Organismal climatology: analyzing environmental variability at scales relevant to physiological stress, *Journal of Experimental Biology,* 213, 6, 995-1003, 0022-0949

Helmuth, B. & Denny, M. W. (2003). Predicting wave exposure in the rocky intertidal zone: do bigger waves always lead to larger forces?, *Limnology and Oceanography,* 48, 1338-1345, 0024-3590

Helmuth, B.; Kingsolver, J. G. & Carrington, E. (2005). Biophysics, physiological ecology, and climate change: does mechanism matter?, *Annual Review of Physiology,* 67, 177-201, 0066-4278

Helmuth, B.; Mieszkowska, N.; Moore, P. & Hawkins, S. J. (2006). Living on the Edge of Two Changing Worlds: Forecasting the Responses of Rocky Intertidal Ecosystems to Climate Change, *Annual Review of Ecology, Evolution, and Systematics,* 37, 1, 373-404, 1543592X

Helmuth, B. S. T. & Hofmann, G. E. (2001). Microhabitats, thermal heterogeneity and patterns of physiological stress in the rocky intertidal zone, *Biological Bulletin,* 201, 374–384, 0006-3185

Hodkinson, I. D. (1999). Species response to global environmental change or why ecophysiological models are important: a reply to Davis et al, *Journal of Animal Ecology,* 68, 6, 1259-1262, 0021-8790

Jones, S. J.; Lima, F. P. & Wethey, D. S. (2010). Rising environmental temperatures and biogeography: poleward range contraction of the blue mussel, Mytilus edulis L., in the western Atlantic, *Journal of Biogeography,* no-no, 1365-2699

Jones, W. E. & Demetropoulos, A. (1968). Exposure to wave action: Measurements of an important ecological parameter on rocky shores on Anglesey, *Journal of Experimental Marine Biology and Ecology,* 2, 1, 46-63, 0022-0981

Koehl, M. (1976). Effects of sea anemones on the flow force they encounter, *Journal of Experimental Biology,* 69, 87-105, 0022-0949

Lewis, J. R. (1964). *The ecology of rocky shores*, English University Press Ltd., 0340213604, London

Lewis, R. (1954). Observations on a high level population of limpets, *Journal of Animal Ecology,* 23, 85–100, 0021-8790

Lima, F. P.; Queiroz, N.; Ribeiro, P. A.; Hawkins, S. J. & Santos, A. M. (2006). Recent changes in the distribution of a marine gastropod, *Patella rustica* Linnaeus, 1758, and their relationship to unusual climatic events, *Journal of Biogeography,* 33, 812-822, 0305-0270

Lima, F. P.; Ribeiro, P. A.; Queiroz, N.; Hawkins, S. J. & Santos, A. M. (2007a). Do distributional shifts of northern and southern species of algae match the warming pattern?, *Global Change Biology,* 13, 2592–2604, 1354-1013

Lima, F. P.; Ribeiro, P. A.; Queiroz, N.; Xavier, R.; Tarroso, P.; Hawkins, S. J. & Santos, A. M. (2007b). Modelling past and present geographical distribution of the marine gastropod *Patella rustica* as a tool for exploring responses to environmental change, *Global Change Biology,* 13, 2065–2077, 1354-1013

Lima, F. P. & Wethey, D. S. (2009). Robolimpets: measuring intertidal body temperatures using biomimetic loggers, *Limnology and Oceanography-Methods,* 7, 347-353, 1541-5856

Menge, B. A. (1976). Organization of the New England Rocky Intertidal Community: Role of Predation, Competition, and Environmental Heterogeneity, *Ecological Monographs,* 46, 4, 355-393, 0012-9615

Mizrahi, T.; Heller, J.; Goldenberg, S. & Arad, Z. (2010). Heat shock proteins and resistance to desiccation in congeneric land snails, *Cell Stress and Chaperones,* 15, 4, 351-363, 1355-8145

Paine, R. T. & Levin, S. A. (1981). Intertidal Landscapes: Disturbance and the Dynamics of Pattern, *Ecological Monographs,* 51, 2, 145-178, 0012-9615

Pan, H.; Qing, Y. & 2010, L. P.-Y. (2010). Direct and indirect measurement of soil suction in the laboratory, *Electronic Journal of Geotechnical Engineering,* 15, 1-14, 1089-3032

Petes, L.; Mouchka, M.; Milston-Clements, R.; Momoda, T. & Menge, B. (2008). Effects of environmental stress on intertidal mussels and their sea star predators, *Oecologia,* 156, 3, 671-680, 0029-8549

Pincebourde, S.; Sanford, E. & Helmuth, B. (2008). Body temperature during low tide alters the feeding performance of a top intertidal predator, *Limnology and Oceanography,* 53, 4, 1562-1573, 0024-3590

Raffaelli, D. & Hawkins, S. J. (1996). *Intertidal Ecology*, Chapman and Hall, 0412299607, London

Santini, G.; Bruschini, C.; Pazzagli, L.; Pieraccini, G.; Moneti, G. & Chelazzi, G. (2001). Metabolic responses of the limpet *Patella caerulea* (L.) to anoxia and dehydration, *Comparative Biochemistry and Physiology - Part A: Molecular & Integrative Physiology,* 130, 1, 1-8, 1095-6433

Schneider, K. R.; Van Thiel, L. E. & Helmuth, B. (2010). Interactive effects of food availability and aerial body temperature on the survival of two intertidal Mytilus species, *Journal of Thermal Biology,* 35, 4, 161-166, 0306-4565

Smaldon, P. R. & Duffus, J. H. (1984). The effects of temperaure, pH and salinity on the maturation of gametes and fertilisation in *Patella vulgata* L, *Journal of Molluscan Studies,* 50, 3, 232-235, 0260-1230

Smee, D. L.; Ferner, M. C. & Weissburg, M. J. (2010). Hydrodynamic sensory stressors produce nonlinear predation patterns, *Ecology,* 91, 5, 1391-1400, 0012-9658

Somero, G. N. (2002). Thermal physiology and vertical zonation of intertidal animals: Optima, limits, and costs of living, *Integrative and Comparative Biology,* 42, 4, 780-789, 1540-7063

Sorte, C. J. B. & Hofmann, G. E. (2004). Changes in latitudes, changes in aptitudes: *Nucella canaliculata* (Mollusca : Gastropoda) is more stressed at its range edge, *Marine Ecology Progress Series,* 274, 263-268, 0171-8630

Sousa, W. P. (1979). Disturbance in Marine Intertidal Boulder Fields: The Nonequilibrium Maintenance of Species Diversity, *Ecology,* 60, 6, 1225-1239, 0012-9658

Sousa, W. P. (1984). Intertidal mosaics: patch size, propagule availability, and spatially variable patterns of succession, *Ecology,* 65, 6, 1918–1935, 0012-9658

Southward, A. J. (1958). Note on the temperature tolerance of some intertidal marine animals in relation to environmental temperatures and geographic distribution., *Journal of the Marine Biological Association of the United Kingdom,* 37, 49-66, 0025-3154

Southward, A. J. (1995). The importance of long time-series in understanding the variability of natural systems, *Helgoländer Meeresuntersuchungen,* 49, 329-333, 0017-9957

Spotila, J. R.; Lommen, P. W.; Bakken, G. S. & Gates, D. M. (1973). A Mathematical Model for Body Temperatures of Large Reptiles: Implications for Dinosaur Ecology, *The American Naturalist,* 107, 955, 391-404, 00030147

Stephenson, T. A. & Stephenson, A. (1949). The universal features of zonation between tidemarks on rocky coasts, *Journal of Ecology,* 38, 289–305, 0022-0477

Wethey, D. S. (1984). Sun and shade mediate competition in the barnacles *Chthamalus* and *Semibalanus* - a field experiment, *Biological Bulletin,* 167, 1, 176-185, 0006-3185

Wethey, D. S. (2002). Biogeography, competition, and microclimate: the barnacle *Chthamalus fragilis* in New England, *Integrative and Comparative Biology,* 42, 872-880, 1540-7063

Wethey, D. S. & Woodin, S. (2008). Ecological hindcasting of biogeographic responses to climate change in the European intertidal zone, *Hydrobiologia,* 606, 1, 139-151, 0018-8158

Yamane, L. & Gilman, S. E. (2009). Opposite responses by an intertidal predator to increasing aquatic and aerial temperatures, *Marine Ecology-Progress Series,* 393, 27-36, 0171-8630